Insulating Biomaterials
N01-NS-62350

Eleventh Quarterly Progress Report
April-June 1999

Submitted to:

Neural Prosthesis Program
National Institutes of Health
National Institute of Neurological
Disorders and Stroke

By the:

Biomedical Microelectronics Laboratory
Biomedical Engineering Center, Massachusetts Institute of Technology
West Roxbury VA Medical Center

Contributors:
David J. Edell, PI
Karen K. Gleason, Chemical Engineering
Bruce C. Larson, Grad Student, Electrical Engineering
Hilton Lewis, Grad Student, Chemical Engineering
Edmund J. Winder, Post Doctoral Fellow, Chemical Engineering
Sean Sexton, Electronics

Introduction

A small fire in a HEPA filter unit in our testing lab did no damage to our instrumentation or test devices, but required temporarily moving the lab and suspending testing for two months. The test systems were then re-calibrated and finally devices were placed under elevated temperature soak testing once again. This distraction delayed other aspects of the work significantly. However, considerable progress had been made in fluorocarbon coatings using a new monomer, and new plasma silicone coatings were also placed under test.

This report focuses on long term saline soak testing of Kapton/Polyimide structures from Troy Nagle's lab at North Carolina State University, and the plasma coating work.

Kapton/Polyimide Structures

Troy Nagle's lab at North Carolina State University prepared five different Kapton based interdigitated electrode arrays to test various approaches to preparation of implantable Kapton based structures. All structures were formed by deposition of gold traces on Kapton substrates followed by coating with an insulator. The insulators used were Dow Corning silicone T-RTV, Dupont Polyimide 2721, Dupont Polyimide 2723, Dupont PC1025, and Dupont Dow3-1753. Initially, samples were dry tested for 3 weeks before the addition of saline to establish a baseline of bulk resistivity. Following addition of saline, many samples survived for an additional 2 weeks. The Dupont Polyimide 2721 coated samples were the most reliable thus far. In QPR10, we modeled the observed trends of degradation of the resistance using a simple linear model. This simple model predicted that the Kapton system would fail in less than one year.

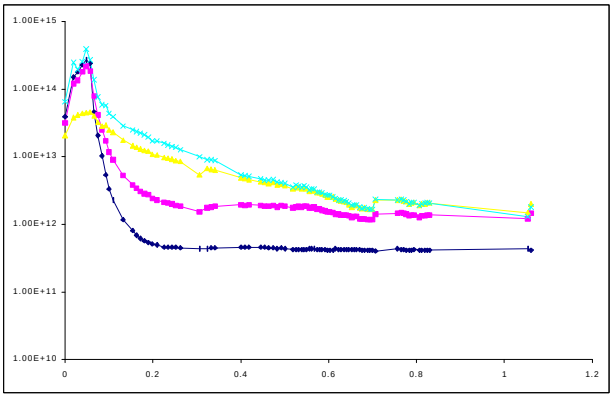

Figure 1: Current data summary of interdigitated electrode arrays of Kapton and Polyimide-2721 from NCSU program.

However, as stated in QPR 10, the prediction was not likely to be reliable because of the many unknowns involved. Subsequent data indicates that the initially observed trend of degradation has changed substantially. Current data from a set of Kapton/Polyimide-2721 interdigitated electrode arrays is shown in Figure 1. The fit used last quarter to predict the ultimate failure of these devices included data from 0.4-0.6 years which was thought to be after the initial transient had decayed away.

However, it is now clear that the initial transient had not fully diminished. Because of the missing data segment, further analysis is not warranted until adidtional data is acquired.

New devices suitable for interconnecting Omnetics Connectors with silicon devices were designed by Jamie Hetke at UM, fabricated by Jason Fiering in Troy Nagle's lab at NCSU, and assembled by Jamie Hetke for evaluation of the entire system. These test devices did not include silicon devices because of a materials interface issue that must also be tested. Half of the devices under test had no exposed traces to test the Kapton-PI2721 system and connector. The other half had exposed traces that were insulated with 353NDT. The substrate Kapton was type VN and was 50um thick. The PI2721 overcoat was 15um thick. Omnetics connectors (A7518-001) were attached with Epoxy Techology H20E and insulated with 353NDT. The traces were about 1cm long with 75um lines and spaces. The device bonding area had traces that were about 3mm long, 120um wide with 30um spaces.

There were four devices of each type, each with four sets of paired test electrodes. They were assembled into test jars and placed under test at the end of the quarter. Initial measurements are encouraging.

Other new tests devices were fabricated by Troy Nagle's lab at NCSU. These devices were constructed with Upilex (polyimide substrate) and PI2721. Some of these devices were overcoated with "A-coat", a plasma deposited dielectric thought to provide moisture barrier properties. These devices were also assembled into test jars and show good performance for a few days under test so far.

The Kapton/PI-2721 system seems to be able to withstand saline soaks for over one year thus far. One of the known failure modes for polyimide in high humidity environments is mechanical degradation. The static soak testing currently evaluates electrical properties in the absence of any mechanical flexing. The planned application for these Kapton ribbon cables is also static, but may involve static bends (ie to fit through the skull onto the brain surface). When it is clear which version of the current devices under soak is likely to be used by UM for interconnecting silicon implants, a new set should be created with static bends in the material to check for stress induced cracking of the coating or substrate during prolonged saline soak testing.

Integrated Circuit Testers

Integrated circuits from the revised run should be available for testing next quarter. Rather than implanting devices that cannot operate at the full device bias of 5 volts, it was decided to wait for the new devices.

Rabbit Testing

All 6 of the remaining implanted rabbits are still doing well. The implanted test devices are comparable to similar devices undergoing long term saline soak testing.

CVD Silicones

16 of the 17 original sets of PPECVD silicone coated silicon substrates are still under test and most of the individual devices are maintaining resistance readings of greater than 1e10 ohms for an exposed area of 0.56cm^2. Since these films are only 1um or so thick, this corresponds to a bulk resistivity of 5e13ohm-cm. This is about right for silicones. These devices have been under test for about one year which is very encouraging.

A new thermal CVD reactor configuration was implemented to provide more uniform depositions. Several monomers are being evaluated to determine if the thermal CVD approach for silicone depositions has merit. Previous attempts resulted in films that were fragile, or had numerous defect inclusions.

CVD Fluoropolymers

Using the new reactor system developed and constructed during the past year, a new set of deposition parameters for fluoropolymer films was developed. The abstract from a paper being submitted for publication follows. The paper is appended to this report.

Growth and Characterization of Fluorocarbon Thin Films Grown from Trifluoromethane (CHF_3) Using Pulsed-Plasma Enhanced CVD

Edmund J. Winder and Karen K. Gleason

1. Abstract

Trifluoromethane (CHF_3) was used as a precursor gas in pulsed-plasma enhanced CVD to deposit fluorocarbon films onto Si substrates. The film composition, as measured by x-ray photoelectron spectroscopy (XPS) of the C 1s peak, was observed to change as the plasma duty cycle was changed by varying the plasma off-time; this offers a route to control the molecular architecture of deposited films. FTIR results indicate that the film is primarily composed of CF_x components, with little or no H incorporation into the film. The rms roughness of the films is extremely low, approaching that of the Si substrate; the low growth rate and consequent high power input/thickness is believed to be partly responsible. CHF_3 produces films with higher % CF_2 compared to other hydrofluorocompound (HFC) monomers (CH_2F_2 and $C_2H_2F_4$). However, the deposition kinetics for all three HFC gases display similar trends. In particular, at a fixed on-time of 10 ms, the deposition rate per pulse cycle reaches a maximum at an off-time of approximately 100 ms.

2. Introduction

Fluorocarbon thin films are an area of active research because they can display a variety of desirable properties not easily obtained with other materials. Specifically, fluorocarbon thin films are being investigated for their use as “low-k” dielectric materials in semiconductor device fabrication,[i] as biocompatible coatings,[ii,iii,iv] as hydrophobic, non-stick coatings,[v] and as low-friction coatings.[vi] Plasma-enhanced CVD (PECVD) is an attractive deposition method for these films because it allows precise thickness control and, because it is solventless, greatly reduces environmental impact compared to traditional coating processes such as spin-on coating.[vii] Pulsed-PECVD has advantages over continuous plasma CVD because the timing of the pulses provides the ability to tune the deposition process.[viii] By varying the plasma duty cycle (the fraction of the cycle time during which the plasma is applied), the deposition can be tailored to make use of either the short-lived ionic species dominant in the plasma, or the longer-lived radical and excited neutral species dominant when the plasma is off; this affects the chemical composition of the resulting film. This improved compositional control is reflected in a variation in the fluorine-to-carbon (F:C) ratio, with a corresponding change in film properties. Additionally, reducing the proportion of plasma on-time reduces the ion bombardment of the growing surface, resulting in a less cross-linked film.

A variety of precursors have been employed to grow fluorocarbon films using PECVD and pulsed-PECVD, including CH_2F_2, $C_2H_2F_4$, and hexafluoropropylene oxide (HFPO).[ix] These precursors were used because they were expected to produce difluorocarbene (CF_2) radicals to varying extents, based on their known thermal and photolytic decomposition pathways.[x] These difluorocarbene radicals are considered important for CF_2 chain growth.[xi] In this paper we report on the growth and characterization of thin fluorocarbon films using another hydrofluorocompound precursor, trifluoromethane (CHF_3), that also produces difluorocarbene by pyrolysis.[xii] Films were grown with this precursor at five different pulsed plasma duty cycles, and subsequently analyzed to determine their composition with x-ray photoelectron spectroscopy (XPS) and fourier-transform infrared spectroscopy (FTIR), their morphology with Atomic Force Microscopy (AFM), and their wetting properties with contact angle measurements.

3. Experimental

Pulsed-PECVD films were grown using five different duty cycles. The plasma on-time was fixed at 10 ms, while off-times of 20, 50, 100, 200, and 400 ms were used. These deposition conditions are referred to as 10/20, 10/50, 10/100, 10/200, and 10/400, respectively. The films were grown on Si substrates placed on the water-cooled ground electrode in a stainless steel capacitively-coupled cylindrical reactor chamber of about 6700 cm^3 volume containing 4"diameter electrodes spaced 1" apart. The plasma was produced by 13.56 MHz rf excitation at a maximum peak power of 280 W while reflected power was minimized with a matching network. The trifluoromethane precursor was 98% pure and used as received from Lancaster. Reactor pressure was kept at one torr during runs, and the feed gas flow rate was 12.5 standard cm^3 (sccm). Deposition times were 15 minutes unless otherwise indicated.

XPS survey scans and high-resolution C 1s spectra were obtained using a Physical Electronics 5200C spectrometer employing a Mg anode operating at 300 W. Further details of the XPS setup and C 1s peak least-squares non-linear regression parameters have previously been provided.[xiii]

Transmission FTIR spectra were obtained using a Nicolet Magna 860 spectrometer equipped with a DTGS KBr detector. A background spectrum taken with a bare Si wafer was subtracted from all of the film spectra. All samples were purged for 20 minutes with dry N_2 prior to collecting spectra in order to remove adsorbed water from the films. For each spectrum, 64 scans were averaged. Although sample film thicknesses varied, the resultant spectra were normalized to a "standard" thickness of 1500 Å to facilitate comparison.

AFM images were obtained at three different scales on each film: 2 μm x 2 μm, 1 μm x 1 μm, and 200 nm x 200 nm. AFM scans were performed in air using a Digital Instruments Nanoscope III Scanning Probe Microscope operating in tapping mode with an etched Si cantilever tip. Although tapping mode does not provide as high a

resolution as contact mode AFM, it greatly reduces the likelihood of sample damage due to dragging the AFM tip across the polymer films.

Surface wetting was investigated by measuring the advancing and retreating contact angles of ≈5 μL water drops on the film surfaces using a Ramé-Hart manual goniometer; measurements were made at three different points on each sample.

Film thicknesses were measured with contact profilometry and single-wavelength ellipsometry. Profilometry was performed with a Tencor P10 Profilometer equipped with a 2 μm radius-of-curvature diamond stylus. Ellipsometry measurements were taken using a Gaertner Scientific L116A ellipsometer operating at a wavelength of 632.8 nm (HeNe laser source) at an incident angle of 70º.

4. Results and Discussion

4.1. GROWTH RATES

As mentioned above, depositions were performed at five different duty cycles. All but the lowest duty cycle, 10/400, were found to be effective in growing fluorocarbon films with this precursor. Although film growth was occasionally observed using a 10/400 duty cycle, it was difficult both to strike and to maintain a stable plasma; successful growth at this set of conditions required frequent tuning of the matching network. Due to the low growth rates and instability of film growth at 10/400, we consider reproducible growth at these conditions to be problematic.

A series of films at the different duty cycles were grown using 15 minute deposition times (60 minutes for the 10/400 film), and growth rates on a per-second and per-cycle basis were calculated using film thicknesses determined via profilometry. These results are summarized in Table 1.

The growth rate per cycle increases slightly as off-time increases up to 100 ms. This is consistent with a significant proportion of deposition occurring during the off-time. As the off-time is increased beyond 100 ms, the growth rate per cycle decreases until it is almost negligible at 10/400 conditions. Similar trends are observed for film growth using other hydrofluorocompound (HFC) precursors. Figure 1 shows the growth rate per cycle as a function of off-time for three different HFC precursors—trifluoromethane (CHF_3), 1,1,2,2-tetrafluoroethane ($C_2H_2F_4$), and difluoromethane (CH_2F_2). The trend in growth rates for CHF_3 is very similar to that for CH_2F_2, which is not surprising given their chemical similarity. Similar mechanisms, such as HF elimination and carbene production, are likely to occur for all three precursors. However, CH_2F_2 does not show the same precipitous drop to near-zero film growth displayed by CHF_3 at 10/400 conditions; the reason for observed difficulty in producing a stable 10/400 CHF_3 plasma is not known.

Although $C_2H_2F_4$ follows the same general trend as the other two precursors, growth rates are much higher for all off-times. The higher growth rates for $C_2H_2F_4$ can be explained in part by the fact that this precursor contains two carbons per molecule, allowing longer fragments to deposit compared to the other precursors, each containing only one carbon.[xiv] Additionally, the pulsed plasma process most likely dissociates the precursor molecules into reactive species with different efficiencies, and this is expected to have an effect on deposition rates.

Compared to the growth rate trends observed for films grown from these three HFCs, the trend in growth rate as a function of plasma off-time is qualitatively different for films grown from HFPO.[xv] For HFPO, using a fixed on period, the growth rate per cycle increases monotonically with off time until approximately 200 ms and then plateaus at constant value as off-time is increased further. This reflects the different processes which are likely to occur. In HFPO, HF elimination is not possible. In addition, the oxygen in this feed gas contributes substantially to the potential pathways available for reaction.

4.2. FILM COMPOSITION

4.2.1. XPS

The relative proportions of different carbon-bonding environments were quantified by analysis of the C 1s XPS peaks. The percentages of these different carbon-bonding environments are reported in Table 2 for the films grown at five different conditions. In general, the 10/20, 10/50, and 10/100 films display very similar chemical makeup, with about 37 % of the carbon contained in CF_2 moieties. The 10/200 film, in contrast, shows a higher percentage of CF_2. This follows a trend observed with pulsed plasma films grown from HFPO, where higher percentages of CF_2 are incorporated with decreasing duty cycle.[xvi] In the limit of no plasma excitation, pyrolytic films grown from HFPO show very high percentages of CF_2, about 90 %.[xvii]

In addition, the fluorine-to-carbon (F:C) ratio and the connectivity number are reported in Table 2. The F:C ratio is calculated from the percentages of different carbon environments as determined from the C 1s XPS by weighting each percentage by the number of F atoms bonded to that carbon. This is expressed in Equation 1:

$$F:C = \frac{(3\times\%CF_3)+(2\times\%CF_2)+(\%CF)}{100} \qquad (1)$$

Bulk PTFE, having a molecular weight above 10^6,[xviii] is essentially composed of CF_2 units and thus has an F:C ratio of 2. In comparing pulsed-plasma fluorocarbon films, films with higher F:C ratios (approaching 2) are considered more “PTFE-like.” The reproducible films grown from CHF_3 show F:C ratios of around 1.4-1.5, with the 10/200

film being the richest in fluorine at F:C = 1.48. The poorly-reproducible 10/400 film displayed a lower F:C ratio of 1.30.

The F:C ratio was also calculated from the atomic concentrations determined during the XPS survey scans of the five films. The F:C ratios calculated in this fashion evidenced the same trend as those calculated from the C 1s peaks, but were slightly higher in value--F:C values ranged from 1.60 for the 10/400 film to 1.82 for the 10/200 film. This disparity between F:C ratios calculated by the two different methods has been observed by other workers.[xix,xx] In some of these cases the F:C values calculated for fluorocarbon films or bulk PTFE from atomic concentrations sometimes substantially exceeded 2; this is impossible for PTFE (since high molecular weight PTFE has an F:C ratio of very nearly 2.0) and suggests using atomic concentrations to calculate F:C ratios is inaccurate. This inaccuracy was tentatively ascribed to errors in the instrument sensitivity factors.

The average connectivity number is a useful measure for estimating the rigidity of amorphous materials.[xxi,xxii] The connectivity number is the average number of network-forming bonds per atom. For our fluorocarbon films, it is calculated in a similar fashion to the F:C ratio, but the different carbon bonding environments are weighted by their ability to bond to other carbons; bonds to F and H are ignored since these are terminal and will therefore not increase the network connectivity. If we also operate under the assumption that the percentage of carbon-carbon double-bonds (i.e. sp^2 C) is minimal, the connectivity number, m, can be taken to be

$$m = \frac{(\%CF_3) + (2 \times \%CF_2) + (3 \times \%CF) + (4 \times \%C - CF)}{100} \qquad (2)$$

The percolation of rigidity for a system should occur at a connectivity value of 2.4; films with m > 2.4 are expected to be rigid (overconstrained), while films with m < 2.4 are expected to be flexible (underconstrained).[xxiii,xxiv] The films studied in this work all show values of m quite close to 2.4.

However, other evidence indicates that these films are brittle. Films of several μm thickness were deposited onto lengths of 75 μm diameter copper wire using the four stable sets of deposition conditions. Short lengths of these coated wires were gently tied into loops about 800 μm in diameter and inspected at various magnifications using an optical microscope. All four coatings exhibited delamination from the wire, indicating a brittle film.

Comparing 10/100 films grown from CHF_3 to 10/100 films grown from other precursor gases reveals a number of interesting facts (Table 3). Trifluoromethane-derived films are more fluorine-rich than films grown from the other two HFC precursors, CH_2F_2 and $C_2H_2F_4$, as evidenced by a substantially higher percentage of CF_2 and a higher calculated F:C ratio. In addition, the connectivity number is substantially lower for CHF_3 films. All three fluorocarbon precursors are inferior at producing fluorine-rich

films when compared to HFPO, which has been shown to produce flexible wire coatings with high % CF_2 and corresponding lower connectivity number of m = 2.1.[xxv] Additionally, films grown from the HFC precursors all display higher proportions of quaternary carbon moieties (C-CF) compared to CF_3 and CF moieties, while films grown from HFPO show roughly equal distributions of CF, CF_3, and C-CF.[xxvi,xxvii]

4.2.2. FTIR

The FTIR spectra of the CHF_3 films provide a complementary means to probe film composition. The spectra of the different CHF_3 films display very similar features, and peak identities were assigned using IR peak information compiled by d'Agostino *et al*.[xxviii] The spectrum for the 10/20 film is shown in Figure 2. The prominent peak centered around 1230 cm^{-1} contains the very strong symmetric and asymmetric CF_2 stretches. The smaller peaks around this region are associated with CF_x moieties. The peak centered at about 1720 cm^{-1} generally indicates C=C and/or C=O functionalities, and is very often observed in pulsed-PECVD fluorocarbon films. The peak around 3500 cm^{-1} represents OH stretching, and is most likely due to a small amount of adsorbed water. The lack of peaks around 2900 cm^{-1} indicates there is little, if any, hydrogen incorporated as C-H in these films. This spectral region is expanded in Figure 3, again for the 10/20 film.

In contrast, films grown from CH_2F_2 and $C_2H_2F_4$ both show C-H stretching peaks, indicating H incorporation into those films. This can be explained by considering the different breakdown mechanisms of these three HFC precursors. CHF_3 is known to break down predominantly into difluorocarbene (CF_2) and hydrofluoric acid (HF).[xxix] Thus, although CHF_3 is a fluorine-rich precursor (F:C = 3) that might be expected to have significant etching capability,[xxx] the presence of hydrogen allows F atoms to be scavenged from the plasma via HF elimination.

CH_2F_2 on the other hand breaks down to principally produce CHF and HF; although F can still be scavenged by HF elimination, CHF incorporation into the film provides a very substantial source of C-H. This helps account for the very low % CF_2 and F:C values observed for these films (see Table 3). The breakdown of $C_2H_2F_4$ is somewhat more complicated; for a plasma on-time of 10 ms, it appears that this compound breaks down roughly equally via two pathways, one producing C_2HF_3 and HF, the other producing C_2F_4 (which can break down to two CF_2's) and H_2.[xxxi] The first route leads to substantial H incorporation, while the second produces CF_2-rich films. This explains why the $C_2H_2F_4$ film is intermediate in % CF_2 and F:C ratio compared to the CH_2F_2 and CHF_3 films (Table 3).

4.2.3. AFM

The films grown from CHF_3 are intriguing in that they exhibit extremely low surface roughness as measured by AFM. Scans performed at three different resolutions for

each film consistently yielded root-mean-square roughnesses of less than a nanometer, approaching the rms roughness value for the Si substrate, which was measured to be 0.53 nm.[xxxii] The 1 μm x 1 μm AFM image of the 10/100 CHF_3 film is shown in Figure 4 and is typical of the AFM images of all the CHF_3 films; no large nodular structures are observed.

The subnanometer rms roughness observed for these films is substantially less than has been observed for comparable films grown from CH_2F_2 and $C_2H_2F_4$.[xxxiii] We believe an important contributing factor to the film roughness is the amount of plasma energy to which the growing film is subjected. This is quantified through the power factor, Q, which is simply the plasma power input per cycle divided by the growth rate per cycle. Figure 5 plots the rms roughness of 10/100 films grown from the three HFC precursors as a function of Q. The slowest growing film (from CHF_3) is subjected to the highest power input and has the smoothest surface; the fastest growing film (from $C_2H_2F_4$) experiences the lowest power input and has the roughest surface.

Table 4 shows the rms roughness and power factor values for the five CHF_3 films, along with the film thickness. No clear trend in roughness with power factor is observed for the CHF_3 films. This may be because the power factor Q may already be above a threshold value, or that differences in surface roughness are hard to quantify so close to the roughness value for the Si substrate material.

Wang and coworkers,[xxxiv] using a mixture of three C_9F_{18} olefins, deposited pulsed-PECVD fluorocarbon films on Si employing average powers similar to those used in this work. These films also displayed low surface roughness, ranging from 0.38 to 1.71 nm, and F:C ratios ranging from 1.18 to 1.72.

4.2.4. Contact Angles

All the films were non-wetting, with advancing contact angles greater than 90°. The 10/20, 10/50, and 10/100 films gave contact angles of 109°; the 10/200 film an angle of 111°; and the 10/400 film an angle of 103°. Bulk PTFE displays a value of 108°.[xxxv]

The contact angle is in general a function of both a surface's composition and roughness.[xxxvi] Since the surface roughness for these films is low and nearly constant, we believe that composition is the more important factor contributing to the small observed differences in contact angles. Increasing the number of fluorine atoms attached to a carbon center increases the group's hydrophobic nature. Increasing the hydrophobicity of the groups making up the surface will increase the contact angle, therefore a film richer in CF_2 and CF_3 groups should evidence a higher contact angle than one richer in CF and quaternary carbon groups. The 10/20, 10/50, and 10/100 films have very similar proportions of CF_x groups, and so not surprisingly yield the same contact angle value. The 10/200 film in comparison has a greater CF_2 fraction but lower CF_3, CF, and C-CF fractions. The net effect is a slightly more fluorinated film, reflected in the slightly higher F:C ratio. This is consistent with the slightly higher

contact angle observed for the 10/200 film. Conversely, the 10/400 film is less fluorinated, with a lower F:C ratio, and the contact angle is lower. Figure 6 displays the advancing contact angles for the CHF_3 films as a function of F:C ratio. These trends are consistent with work on pulsed-PECVD fluorocarbon films done by Wang *et al*[xxxvii] who observed advancing contact angles with water to substantially increase as the F:C ratio increased, even while surface roughness slightly decreased.

Slightly smaller contact angles of 101° and 107° were observed for 10/100 films grown from CH_2F_2 and $C_2H_2F_4$, respectively. These films are substantially less fluorinated than the CHF_3 films, but they are rougher (R_{rms}=12 and 22 nm, respectively). Films grown from HFPO, in contrast, are more fluorinated and display a slightly higher contact angle, 113°, than the CHF_3 films.[xxxviii]

5. Conclusion

A series of fluorocarbon films was deposited onto Si substrates via pulsed plasma enhanced CVD using trifluoromethane (CHF_3) as the source gas. Film compositions (as measured by changes in CF_x proportions) varied as the plasma duty cycle was changed (by varying the plasma off-time at a fixed on-time of 10 ms). The variation in CF_2 percentage was less pronounced for this precursor than has been observed for films grown from HFPO under similar conditions. We believe this is due to CHF_3 decomposition being dominated by one pathway, breaking down predominantly to produce CF_2 and HF, therefore making it difficult to alter ratios of these two gas-phase species via plasma conditions.

The films display a F:C ratio of 1.4-1.5, substantially higher than observed for films grown from two other HFC precursors, CH_2F_2 (film F:C = 0.60) and $C_2H_2F_4$ (film F:C = 0.91); films from HFPO show a higher ratio (film F:C = 1.78). In addition, the average connectivity number for CHF_3 films is about 2.4, considered the value where percolation of rigidity can occur and films can become flexible; this is significantly lower than the average connectivity value observed for the other HFC precursors. However, optical microscopy of loops of coated wires reveal delamination of the films, indicating the deposited films are rigid. Films grown from HFPO have displayed lower average connectivity numbers (m = 2.2) and flexible characteristics when coated onto wires and tied into loops.

FTIR spectra indicate that the films are essentially composed of CF_x species, and that there is very little C-H incorporation into films grown using CHF_3 at any of the plasma conditions.

Films grown from CHF_3 are extremely smooth, with rms roughnesses (determined by AFM) on the order of the roughness of the Si wafer substrate, about 0.5 nm. We believe this is due in large part to the relatively low film growth rates, which result in a large amount of plasma power being applied to the growing film.

Advancing contact angles with water are close to 108°, the value for bulk PTFE. A very small trend in contact angle with varying duty cycle is observed, with more fluorinated (higher F:C ratio) films displaying higher contact angles, i.e. exhibiting more nonwetting, hydrophobic character.

6. Acknowledgment

We gratefully acknowledge the NIH for support of this work under contract NO1-NS-3-2301. This work made use of MRSEC Shared Facilities supported by the National Science Foundation under Award No. DMR-9400334.

6.1.1.1.Tables

Plasma conditions	Growth rate (Å/s)	Growth rate (Å/cycle)
10/20	15.1	0.454
10/50	10.1	0.606
10/100	5.53	0.608
10/200	1.09	0.228
10/400	0.0839	0.0344

Table 1. Growth rates of fluoropolymer films grown from CHF_3 at various plasma conditions. Rates are shown on a per-time and per-cycle basis.

Plasma conditions	$\%CF_3$	$\%CF_2$	%CF	%C-CF	F:C	Connectivity Number
10/20	14.4	37.3	23.2	25.0	1.41	2.41
10/50	15.6	37.3	20.8	26.3	1.42	2.48
10/100	15.8	36.5	21.8	25.9	1.42	2.46
10/200	11.6	47.7	17.6	23.1	1.48	2.40
10/400	14.7	32.2	21.7	31.3	1.30	2.55

Table 2. Summary of C 1s XPS analysis of films grown from CHF_3 at 5 different sets of conditions. Percentages of the four different carbon bonding environments are listed. The F:C ratio and average connectivity number are calculated from the percentages, using the weighting methods of Equations (1) and (2), respectively.

Precursor	$\%CF_2$	F:C	Connectivity Number
CF_3H	36	1.42	2.46
CH_2F_2	12	0.60	3.40
$C_2H_2F_4$	21	0.91	3.09
HFPO	55	1.78	2.22

Table 3. $\%CF_2$, F:C ratio, and connectivity number for 10/100 films grown from four different precursors. CHF_3 produces films that are more PTFE-like than the other fluorocarbon precursors, but not as PTFE-like as HFPO films. Data for CH_2F_2 and $C_2H_2F_4$ films from [1]; data for HFPO is for a 10/90 film from [2]

Conditions	R_{rms} (nm)	Q (J/nm)	Film thickness (nm)
10/20	0.786	61.7	1365
10/50	0.685	46.2	911
10/100	0.632	46.1	498
10/200	0.593	123	98
10/400	0.756	814	30

Table 4. Roughness, power factor, and thickness of CHF_3 films grown at different plasma conditions. Values reported are for 1 μm x 1 μm scans; values obtained from 2 μm x 2 μm and 200 nm x 200 nm scans are very similar.

Figures

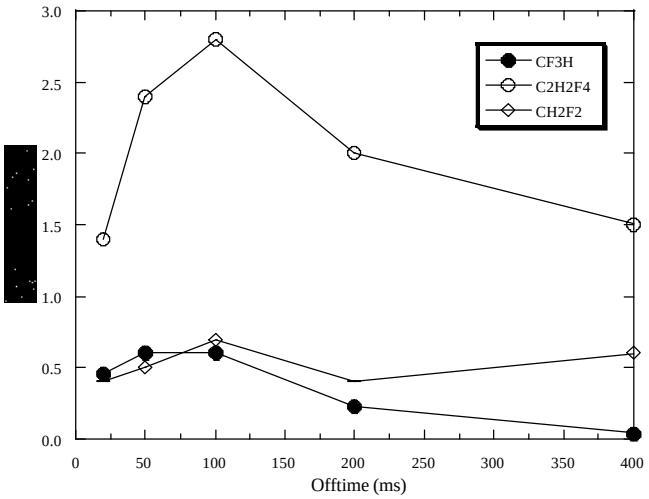

Figure 1. Growth rate per cycle as a function of plasma off-time for three different fluorocarbon precursors. Plasma on-time for all depositions was fixed at 10 ms. Data for CH_2F_2 and $C_2H_2F_4$ taken from [1]

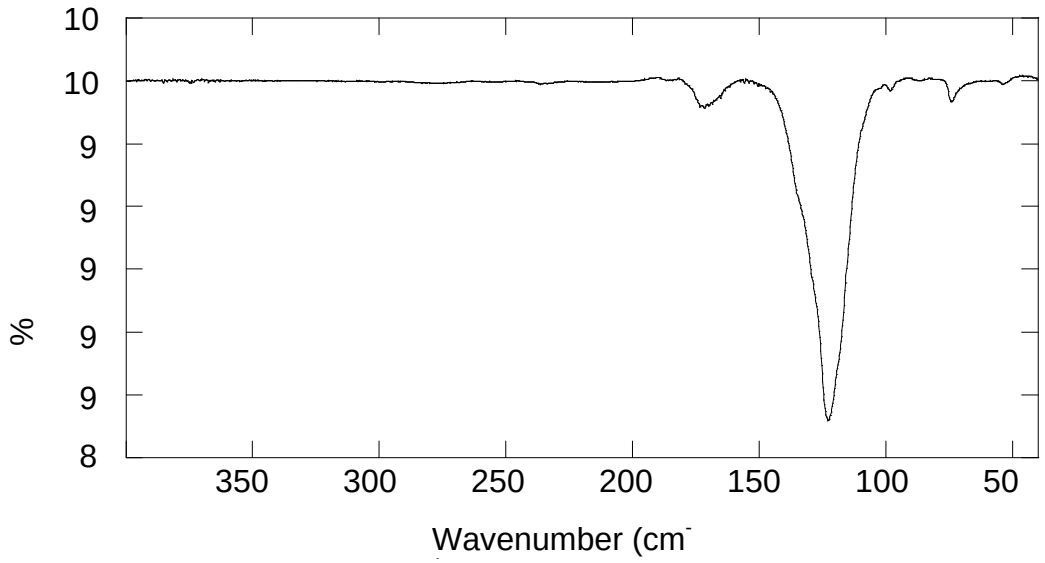

Figure 2. FTIR spectrum of 10/20 CHF_3 film. Main features are CF, CF_2, and CF_3 peaks. OH stretching around 3550 cm^{-1} is most likely due to adsorbed water. Spectra for CHF_3 films at lower duty cycles are similar but noisier due to lower film thickness.

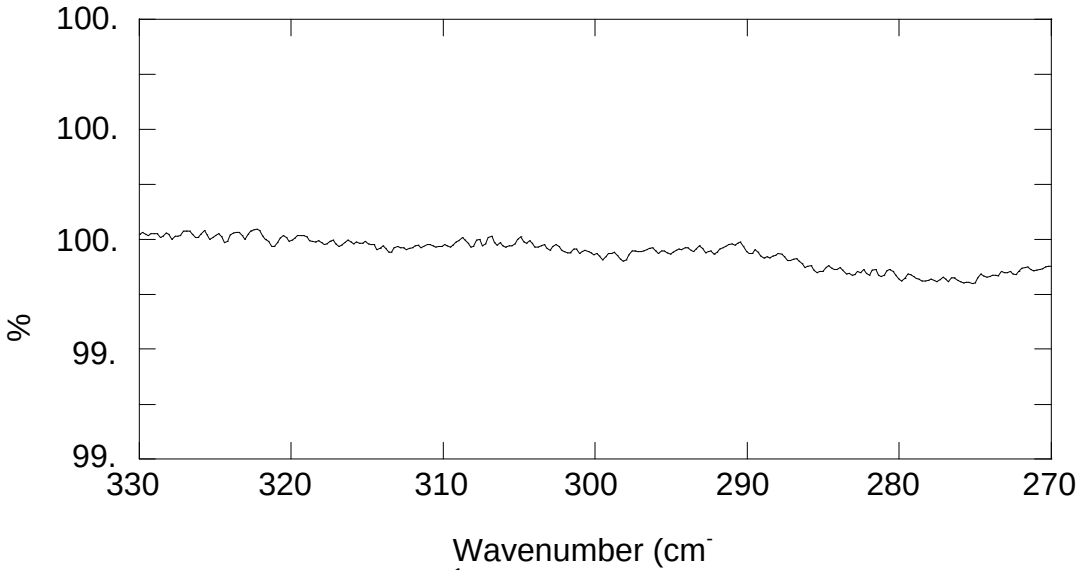

Figure 3. Expansion of FTIR spectrum of Figure 2 detailing CH_x stretching region of 10/20 CHF_3 film. No significant C-H incorporation into the film is observed. Spectra of other CHF_3 films are similar.

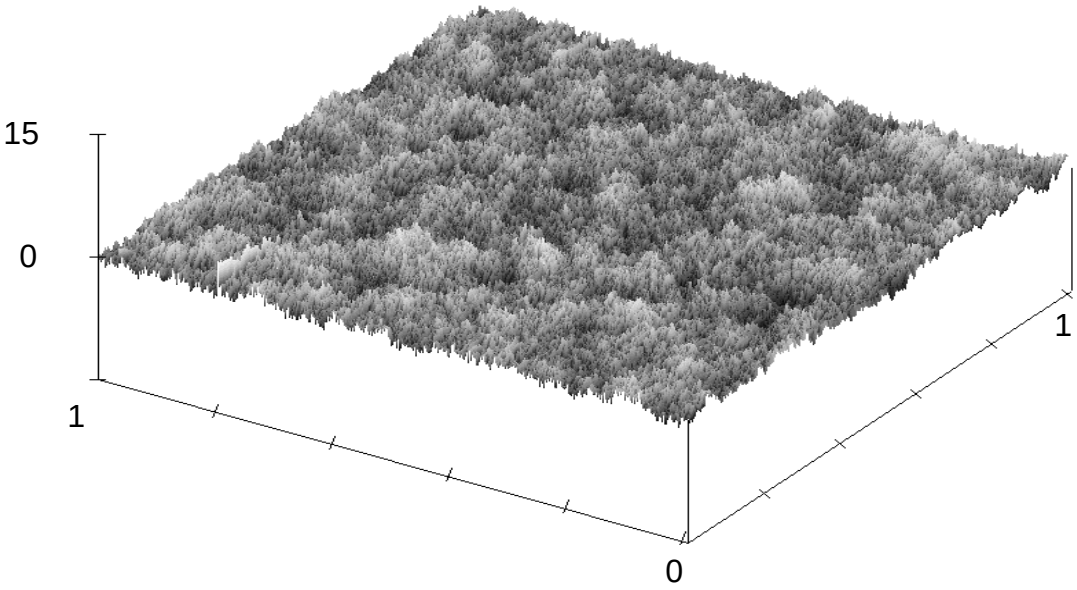

Figure 4. AFM image of 10/100 film grown from CHF_3. Film is about 5000 Å thick; area shown is 1 μm x 1 μm. Images of the other CHF_3 films are similar in appearance.

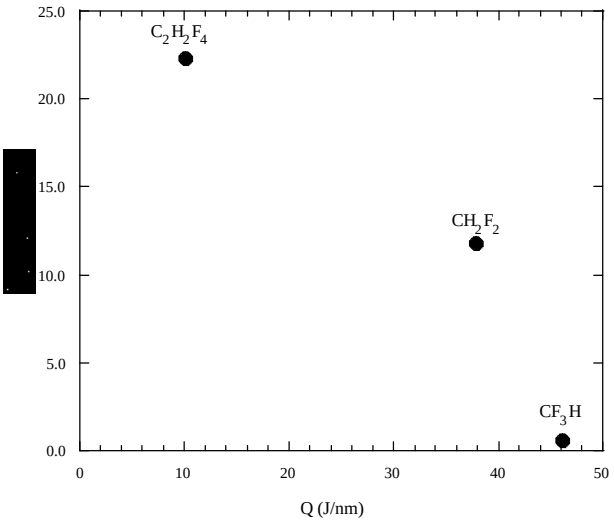

Figure 5. Surface roughness as a function of power factor, Q, for 10/100 films grown using three different fluorocarbon precursors. Data for CH_2F_2 and $C_2H_2F_4$ are taken from [3]

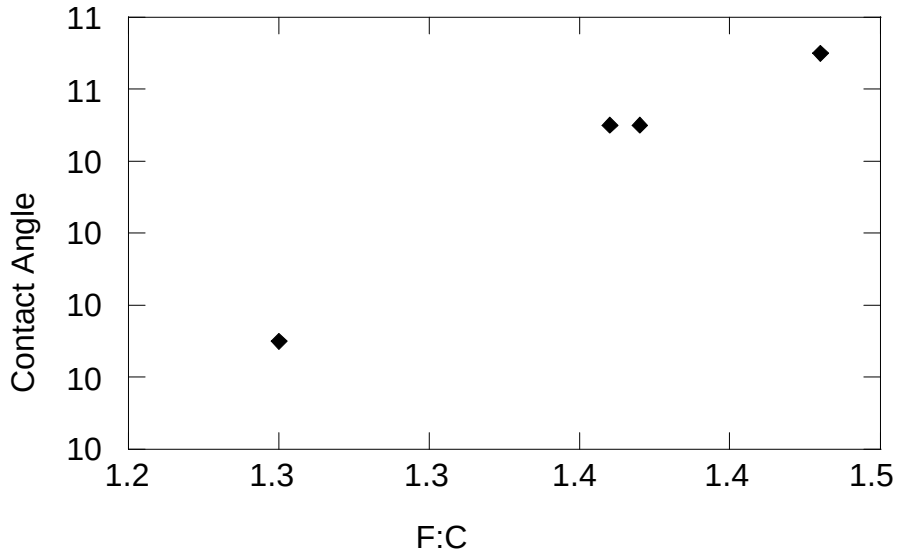

Figure 6. Advancing contact angle as a function of F:C ratio for films grown from CHF_3 (see also Table 2).

Labelle, C. B.; Gleason, K. K. *J. Vac. Sci. Technol. A* **1999**, *17*, 445.
Limb, S. J. Pulsed Plasma Enhanced and Pyrolytic Chemical Vapor Deposition of Fluorocarbon Biopassivation Coatings. PhD, Massachusetts Institute of Technology, 1997.
Labelle, C. B.; Gleason, K. K. *J. Appl. Polym. Sci.* **in press**.

---

[i] a) Endo, K.; Tatsumi, T. *J. Appl. Phys.* **1995**, *78*, 1370.
b) Endo, K. *MRS Bulletin* **1997**, *22*, 55.
c) Labelle, C. B.; Limb, S. J.; Gleason, K. K.; Burns, J. A. *Proc. of Third International Dielectrics for ULSI Multilevel Interconnection Conference (DUMIC)* **1997**, 98.
[ii] Limb, S. J.; Gleason, K. K.; Edell, D. J.; Gleason, E. F. *J. Vac. Sci. Technol. A* **1997**, *15*, 1814.
[iii] Yasuda, H.; Gasicki, M. *Biomaterials* **1982**, *3*, 68.
[iv] Gumbotz, W. B.; Hoffman, A. S. *CRC Critical Reviews in Biocompatibility* **1987**, *4*, 1.
[v] Grischke, M.; Bewilogua, K.; Trojan, K.; Dimigen, H. *Surfaces and Coatings Technology* **1995**, *74-75*, 739.
[vi] a) Pittman, A. G. Surface Properties of Fluorocarbon Polymers. In *Fluoropolymers*; Wall, L. A., Ed.; John Wiley and Sons: New York, 1972; Vol. XXV; pp 419.
b) Momose, Y.; Takada, T.; Okazaki, S. "CF4 and C2F6 Plasma Fluorination of Hydrocarbon and Fluorocarbon Polymers"; Polymeric Materials Science and Engineering, 1987, Denver, CO.
[vii] Labelle, C. B.; Gleason, K. K. "Environmental, Safety, and Health Issues associated with Low Dielectric Constant Films Grown by Chemical Vapor Deposition"; 1st International Symposium on Environmental Issues with Materials and Processes for the Electronic and Semiconductor Industries, 1998, San Diego.
[viii] a) Savage, C. R.; Timmons, R. B.; Lin, J. W. *Chemical Materials* **1991**, *3*, 575.
b) Limb, S. J.; Lau, K. K. S.; Edell, D. J.; Gleason, E. F.; Gleason, K. K. *Plasmas and Polymers* **In press**.
[ix] a) Labelle, C. B.; Lau, K. K. S.; Gleason, K. K. *Mater. Res. Soc. Symp.* **1998**, *511*, 75.
b) Limb, S. J.; Edell, D. J.; Gleason, E. F.; Gleason, K. K. *submitted to Chem. Mater.* **1997**.
[x] $C_2H_2F_4$: a) Millward, G. E.; Hartig, R.; Tschuikow-Roux, E. *J. Phys. Chem.* **1971**, *75*, 3195.
b) Burgess, D. R., Jr.; Zachariah, M. R.; Tsang, W.; Westmoreland, P. R. *Progress in Energy Combustion Science* **1996**, *21*, 453..

CH_2F_2: Burgess, D. R., Jr.; Zachariah, M. R.; Tsang, W.; Westmoreland, P. R. *Progress in Energy Combustion Science* **1996**, *21*, 453.
[xi] Limb, S. J.; Labelle, C. B.; Gleason, K. K.; Edell, D. J.; Gleason, E. F. *Appl. Phys. Lett.* **1996**, *68*, 2810.
[xii] a) Schug, K. P.; Wagner, H. G.; Zabel, F. *Ber. Bunsenges. Phys. Chem.* **1979**, *83*, 167.
b) Hidaka, Y.; Nakamura, T.; Kawano, H. *Chem. Phys. Lett.* **1991**, *187*, 40.
[xiii] Limb, S. J.; Edell, D. J.; Gleason, E. F.; Gleason, K. K. *J. Appl. Polym. Sci.* **1998**, *67*, 1489.
[xiv] Labelle, C. B.; Gleason, K. K. *J. Vac. Sci. Technol. A* **1999**, *17*, 445.
[xv] Limb, S. J. Pulsed Plasma Enhanced and Pyrolytic Chemical Vapor Deposition of Fluorocarbon Biopassivation Coatings. PhD, Massachusetts Institute of Technology, 1997.
[xvi] Limb, S. J.; Lau, K. K. S.; Edell, D. J.; Gleason, E. F.; Gleason, K. K. *Plasmas and Polymers* **In press**.
[xvii] Limb, S. J.; Lau, K. K. S.; Edell, D. J.; Gleason, E. F.; Gleason, K. K. *Plasmas and Polymers* **In press**.
[xviii] *Organofluorine Chemicals and their Industrial Applications*; Banks, R. E., Ed.; John Wiley and Sons: New York, NY, 1979.
[xix] Wang, J.-H.; Chen, J.-J.; Timmons, R. B. *Chem. Mater.* **1996**, *8*, 2212.
[xx] Clark, D. T.; Shuttleworth, D. J. *J. Polym. Sci. Polym. Chem. Ed.* **1980**, *18*, 27.
[xxi] He, H.; Thorpe, M. F. *Physical Review Letters* **1985**, *54*, 2107.
[xxii] Dohler, G. H.; Dandoloff, R.; Bilz, H. *J. Non-Cryst. Solids* **1980**, *42*, 87.
[xxiii] He, H.; Thorpe, M. F. *Physical Review Letters* **1985**, *54*, 2107.
[xxiv] Dohler, G. H.; Dandoloff, R.; Bilz, H. *J. Non-Cryst. Solids* **1980**, *42*, 87.
[xxv] Limb, S. J.; Gleason, K. K.; Edell, D. J.; Gleason, E. F. *J. Vac. Sci. Technol. A* **1997**, *15*, 1814.
[xxvi] Labelle, C. B.; Gleason, K. K. *J. Vac. Sci. Technol. A* **1999**, *17*, 445.
[xxvii] Limb, S. J.; Lau, K. K. S.; Edell, D. J.; Gleason, E. F.; Gleason, K. K. *Plasmas and Polymers* **In press**.
[xxviii] d'Agostino, R.; Cramarossa, F.; Fracassi, F. Plasma Polymerization of Fluorocarbons. In *Plasma Deposition, Treatment, and Etching of Polymers*; d'Agostino, R., Ed.; Academic Press, Inc.: San Diego, 1990; pp 95.
[xxix] a) Schug, K. P.; Wagner, H. G.; Zabel, F. *Ber. Bunsenges. Phys. Chem.* **1979**, *83*, 167.
b) Hidaka, Y.; Nakamura, T.; Kawano, H. *Chem. Phys. Lett.* **1991**, *187*, 40.
[xxx] d'Agostino, R.; Cramarossa, F.; Fracassi, F. Plasma Polymerization of Fluorocarbons. In *Plasma Deposition, Treatment, and Etching of Polymers*; d'Agostino, R., Ed.; Academic Press, Inc.: San Diego, 1990; pp 95.
[xxxi] Labelle, C. B.; Karecki, S. M.; Reif, L. R.; K.K. Gleason. *J. Vac. Sci. Technol. A* **submitted**.
[xxxii] Labelle, C. B.; Gleason, K. K. *J. Appl. Polym. Sci.* **in press**.
[xxxiii] Labelle, C. B.; Gleason, K. K. *J. Appl. Polym. Sci.* **in press**.
[xxxiv] Wang, J.-H.; Chen, J.-J.; Timmons, R. B. *Chem. Mater.* **1996**, *8*, 2212.
[xxxv] Zisman, W. A. *Adv. Chem. Ser.* **1964**, *43*.
[xxxvi] Adamson, A. W.; Gast, A. P. *Physical Chemistry of Surfaces*, 6th ed.; John Wiley and Sons: New York, 1997.
[xxxvii] Wang, J.-H.; Chen, J.-J.; Timmons, R. B. *Chem. Mater.* **1996**, *8*, 2212.
[xxxviii] Labelle, C. B.; Gleason, K. K. *J. Appl. Polym. Sci.* **in press**.